ALMA Memo # 394

ALMA band 9 optical layout

A. Baryshev, W. Wild
NOVA/SRON Groningen, Sept-2001

Table of Contents

1 Abstract/Introduction 1
2 Design concept 1
2.1 Corrugated and diagonal horn representation 1
2.1.1 Equivalent diagonal horn 2
2.2 Compensation of distortion in pair of elliptical mirrors 3
2.3 Frequency independent coupling between horn and telescope beam 6
3 Proposed layout 8
3.1 ALMA band 9 corrugated and diagonal horn design 8
3.2 ALMA band 9 signal path optical layout 9
4 Mirror alignment tolerances 10
5 Conclusions 12

1 Abstract/Introduction

In this report a mm wave optics prototype for an Atacama Large Millimeter Array (ALMA) receiver cartridge is discussed. Mainly the ALMA frequency band 9 (602-720 GHz) is considered. However the same design approach is applicable to the receiver optics of any other ALMA bands.
The high frequency cartridges (bands 7-10) have been decided to have no intermediate optics between the telescope secondary mirror and the cartridge cold optics. (See notes of Tucson optics meeting). Consequently, in the optical design of band 9 cartridge full signal path with all focusing elements are considered as free design parameters.
In this report a concept of choosing and optimizing these parameters is discussed. The design starts from an optimal corrugated and diagonal horn field representation. A possibility of distortion compensation by a pair of ellipsoidal mirrors is discussed. A concept of frequency independent radiation coupling between the horn and the Cassegrain telescope system is presented. An expression for parameters of two elliptical mirrors giving rise to frequency independent matching of the horn to the telescope is given.
A practical corrugated horn for signal path of mixer and a practical diagonal horn for local oscillator (LO) part of mixer are proposed. Based on the horn and the ALMA prototype antenna design a two-mirror layout for ALMA band 9 is proposed.
The alignment accuracy of optical components within the cartridge is considered. The alignment accuracy between the cartridge and the secondary mirror is also considered.

2 Design concept

In this part a few theoretical facts, used in the following practical design, are discussed.

2.1 Corrugated and diagonal horn representation

The essential part of the quasi-optical design is the feeds. The corrugated horn has been shown to have a very good Gaussian beam over at least 1.5:1 frequency range. The possibility of machining of these horns has been shown for frequencies at least up to 1 THz. The coupling efficiency to the zero order Gaussian beam can exceed 98 % for this type of horn. That is why we will use it as feed in the signal path of band 9.

Throughout this report we will be using the following expression for the electrical field distribution over the horn aperture:

$$E_{ch} = \frac{1.08684}{a} J_0\left(\frac{2.405 \cdot r}{a}\right) \cdot Exp\left(\frac{-j\pi r^2}{\lambda R_h}\right), \quad (1)$$

where r is radius over the horn aperture, a is the radius of horn aperture and R_h is the horn slant length. We do not consider the cross polarization in this representation, so the formula is given for main polarization. Expression (1) is slightly different from the one given in [1]. It was modified for normalization purpose such as the beam coupling given by:

$$A = \left| \int_0^a E_a E_b^* 2\pi r dr \right|^2 . \quad (2)$$

is equal to 1 when $E_b = E_a = E_c$. The coupling between the horn and the fundamental Gaussian beam is then simply given by (2) where Gaussian beam distribution is used for E_a and E_{ch} is used for E . In this design we will use the fact that the radius of curvature of the beam in the horn aperture is very close to horn slant length. It can be found that Gaussian beam radius at the corrugated horn aperture should be $w = 0.644a$ (for aperture illumination taper 8.6 dB). Given this condition the optimum Gaussian beam will have a waist size w_0 and distance from horn aperture (towards horn apex) z are given in following expressions:

$$w_0 = \frac{w}{\sqrt{1+\pi\left(\frac{w^2}{\lambda R_h}\right)^2}}, \quad (3)$$

$$z = \frac{R_h}{1+\left(\frac{\lambda R_h}{\pi w^2}\right)^2} . \quad (4)$$

More than 99% of power in the Gaussian beam with parameters given in (3) and (4) is coupled into the corrugated horn. For the geometrical optics limit ($\lambda \to 0$ in (4)) we find that geometrical optics image is located in the horn apex. This fact will be used for building an optical system for band 9 using geometrical optics.

2.1.1 Equivalent diagonal horn

The band 9 mixers will use a quasi-optical LO injection. We propose to use the diagonal horn as a feed for the LO source. There are several reasons for this choice: the antenna beam pattern of such a horn is reasonably good, the optimum Gaussian beam coupling for this type of horn can be as high as 84 % and – quite important – a diagonal horn is much easier to produce than a corrugated horn. The overall coupling between optimum corrugated horn and optimum diagonal horn will be about 82 % that is enough to efficiently couple LO signal in a mixer.

The electrical field in the aperture plane of a diagonal horn is described by following equations:

$$E_{II} = \frac{1}{\sqrt{2}}\left[\vec{x} \cdot Cos\left(\frac{\pi \cdot y}{a}\right) + \vec{y} \cdot Cos\left(\frac{\pi \cdot x}{a}\right)\right] \cdot Exp\left(\frac{-j \cdot \pi \cdot (x^2+y^2)}{\lambda \cdot R_h}\right), \quad (5)$$

$$E_{\perp} = \frac{1}{\sqrt{2}}\left[\vec{x} \cdot Cos\left(\frac{\pi \cdot y}{a}\right) - \vec{y} \cdot Cos\left(\frac{\pi \cdot x}{a}\right)\right] \cdot Exp\left(\frac{-j \cdot \pi \cdot (x^2+y^2)}{\lambda \cdot R_h}\right), \quad (6)$$

$$|x| \le \frac{a}{2};\ |y| \le \frac{a}{2}, \quad (7)$$

where E_{II} is the co-polar component (along axis v), $E_{\perp}$ is the cross-polar component, a is aperture size, R_h is horn slant length, and $\vec{x}$, $\vec{y}$ are orts of coordinate system as shown in Figure 2.1.

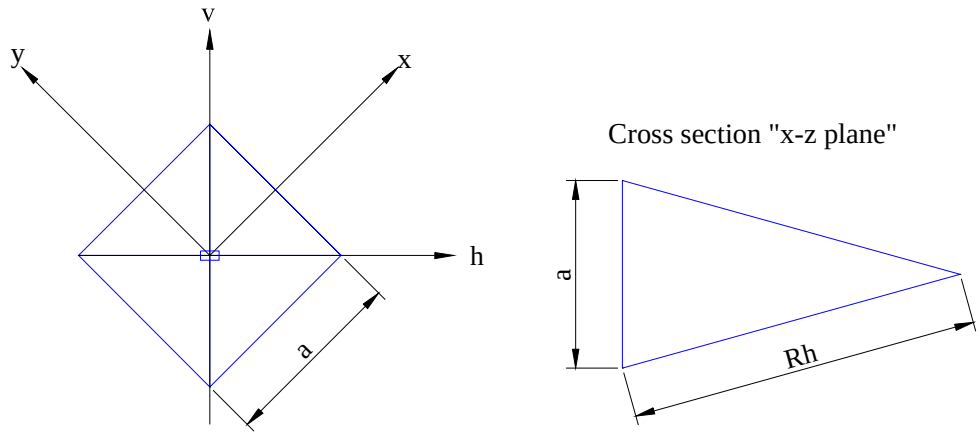

Figure 2.1 Diagonal horn geometry.

An optimum Gaussian beam coupling of ~ 84 % to this type of horn is achieved when the fundamental mode beam radius $w = 0.43 \cdot a$. The beam radius of curvature in this case is also equal to R_h. The waist position and size can be defined by the same set of equations (3) and (4).
As it will be shown in sections 2.2, 0 it is especially advantageous if corrugated and diagonal horns to match has the same optimal fundamental mode beam waist sizes and positions. This can be achieved if the diagonal horn size a_d is related to the corrugated horn radius a_c as $a_d = 1.5 \cdot a_c$ and slant lengths of both radiators are equal. This symmetry allows to achieve frequency independent coupling and to avoid beam distortions when using two identical elliptical mirrors to couple one horn to another.

2.2 Compensation of distortion in pair of elliptical mirrors

Cold reflective optics will be used to match the telescope beam to the mixer horn. Since the telescope beam coming from the secondary and the horn beam have a different F-ratios (in geometrical optics limit) and mixer can not be mounted in the focal plane at least one elliptical mirror is required for matching. A Gaussian beam telescope is often used for frequency independent matching. This type of system requires at least two optical elements. The telescope secondary mirror can be used as the first optical element (NRAO optical design proposal) but to allow more freedom in designing and to enable different matching scheme (see Section 2.3) we consider here a system of two elliptical mirrors following between telescope focal plane and mixer horn. The beam distortion produced by two mirrors is analysed in this section in geometrical optics limit.
The layout of such a system is presented in Figure 2.2. This layout is used for matching scheme that is described in Section 2.3.

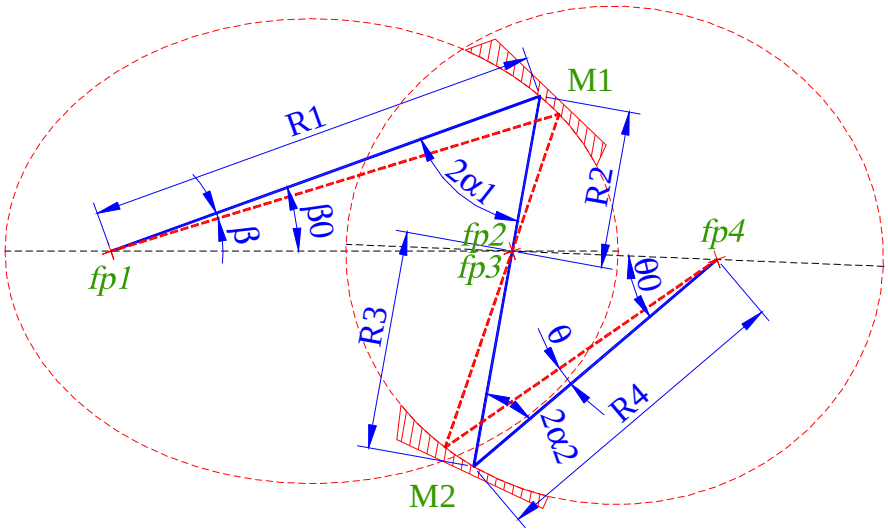

Figure 2.2 Optical layout with two elliptical mirrors and some and parameters (see text for details). Chief ray is given by blue solid line, deflected ray is given by red dashed line.

Two elliptical mirrors M1 and M2 with focal points *fp1*, *fp2* and *fp3*, *fp4* respectively are arranged in such a way that *fp2* coincides with *fp3*. Telescope focal plane is located at *fp1*. Mixer horn is located at *fp4*. The chief ray is shown by bold solid line. Distances ($R1, R2, R3, R4$) are usually defined in optical train calculations and are chosen for optimal matching. Two bending angles ($\alpha 1, \alpha 2$) are also required to define an ellipse shape. These two angles are usually chosen as small as possible in order to minimize a distortion (L_{dist}) and cross-polarization (L_{cp}) loss in the system. This loss for fundamental Gaussian beam mode can be estimated using following equations [1, 2]:

$$L_{dist} = \frac{w^2 \tan^2(\alpha)}{8 \cdot f^2}, \tag{8}$$

$$L_{cp} = \frac{w^2 \tan^2(\alpha)}{4 \cdot f^2}, \tag{9}$$

where w is a Gaussian beam radius at the mirror, α is a bending angle and f is the focal distance of a mirror. In the worst case the losses from two mirrors sum up. However for some configurations (like one shown in Figure 2.2) two mirrors can compensate each other. From (8), (9) it is seen, that one can expect full compensation if two mirrors are identical and beam radii are the same.

In order to investigate the distortion compensation we consider the angle magnification of the system in geometrical optics limit. This magnification M for small angles is given by:

$$\mathrm{M} = \left(\frac{d\theta}{d\beta} \right)^{-1}, \tag{10}$$

where θ and β are output and input angles of the system as shown in Figure 2.2. For the chief ray this magnification is simply multiplication of magnifications of mirrors: $\mathrm{M}^0 = \mathrm{M1} \cdot \mathrm{M2}$, where $\mathrm{M1} = R2/R1$ and $\mathrm{M2} = R4/R3$. Exact expression for (10) can be derived taking into account geometrical shape of ellipses given by initial parameters: $R1, R2, R3, R4, \alpha 1, \alpha 2$. After algebraic transformations, which we will not present here, it can be shown that M is only function of $\mathrm{M}(\mathrm{M1}, \mathrm{M2}, \alpha 1, \alpha 2, \beta)$. Furthermore, it can be shown, that if $\alpha 1$ and $\alpha 2$ are related by the following expression [3]:

$$\alpha 2 = ArcTan\left(\frac{(1+\mathrm{M1}) \cdot Tan(\alpha 1)}{\left(1 + \frac{1}{\mathrm{M2}}\right)} \right), \tag{11}$$

M becomes a function of $\mathrm{M}(\mathrm{M}^0, \beta)$ and the magnification deviation $\left|\mathrm{M}(\mathrm{M}^0, \beta) - \mathrm{M}^0\right|$ is minimized. Distortion becomes also symmetrical with respect to the chief ray i.e. $\mathrm{M}(\mathrm{M}^0, \beta) = \mathrm{M}(\mathrm{M}^0, -\beta)$ for all realizable input angles.

For the special case of $\mathrm{M}^0 = 1$ the system magnification M becomes independent of input angle β and $\alpha 1 = \alpha 2$. This case represents that it is possible to match two similar radiators with two elliptical mirrors with the same parameters regardless of values for bending angles $\alpha 1 = \alpha 2$. Distortion in this mirror pair appears to be compensated for all bending angles. For this purpose we aim for having the same horns on a LO oscillator last stage and a mixer.

In the case of the band 9 signal path M^0 is not equal to unity. However, if ellipses bending angles are related by equation (11) the distortions are minimized and output beam becomes symmetrical. This fact is illustrated in Figure 2.3, where the normalized magnification $\mathrm{M}(\mathrm{M1}, \mathrm{M2}, \alpha 1, \alpha 2, \beta)/(\mathrm{M1} \cdot \mathrm{M2})$ is plotted with respect to the input angle β and bending angle $\alpha 1$ provided that bending angle $\alpha 2$ is chosen to be for $\alpha 1 = 30^\circ$ optimal using equation (11). One can see that for the optimum input angle of 30° the distortions are minimized, beam is symmetrical and magnification errors are minimized to 1 % for input angles of ±7 °. The beam contained by these input angles carries > 99 % of fundamental Gaussian mode power for F/#8 input beam in 600-720 GHz band. Magnifications $\mathrm{M1}$ and $\mathrm{M2}$ are taken from proposed layout in section 3.2.

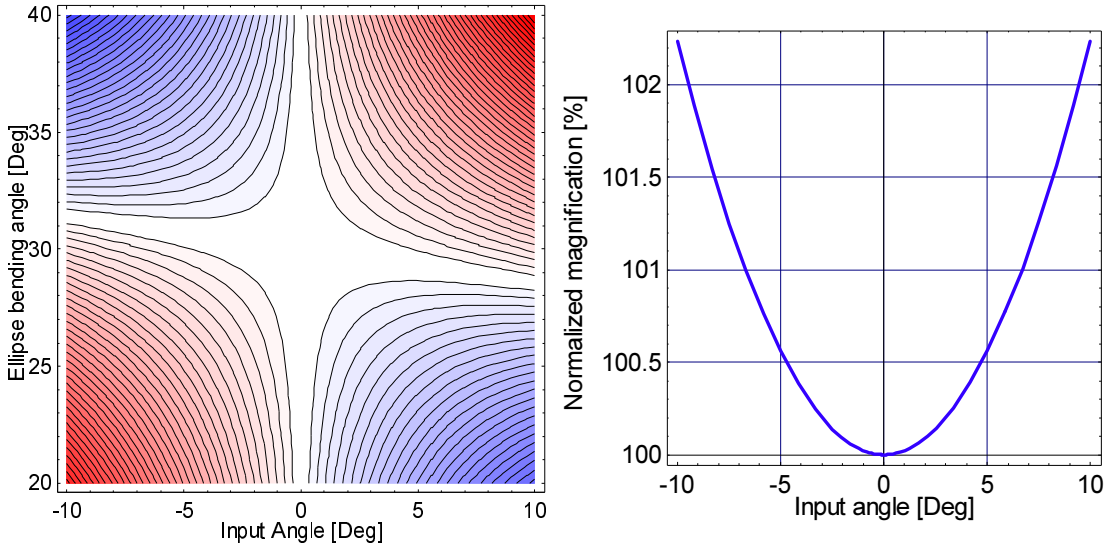

Figure 2.3 Normalized magnification of two-mirror system with respect to input angle and bending angle of the first mirror. a) Contour plot, space between contours is 0.5 %. 100 % Contour is omitted. Red color indicates values >100.5 %, blue color shows values <99.5 %. b) Cross section of the contour plot for $\alpha 1 = 30°$ (optimum angle)

The above results are obtained for geometrical optics limit. The same property of distortion compensation should be valid for fundamental Gaussian mode distortion. It means that higher order modes launched by the first mirror are partly coupled back to the fundamental Gaussian mode at the second mirror. For calculation of distortion loss we can use equation (8) for each mirror and subtract the results, substituting beam radiuses taken from an optical train calculation:

$$L_{dist} = \left| \frac{w_1^{\,2} \tan^2(\alpha 1)}{8 \cdot f_1^{\,2}} - \frac{w_2^{\,2} \tan^2(\alpha 2)}{8 \cdot f_2^{\,2}} \right|. \qquad (12)$$

The loss given by equation (12) appears to be fully minimized if relation (11) is used for angles and frequency is tending to infinity. A correction appears to be necessary for lower frequency because beam sizes become frequency dependent.

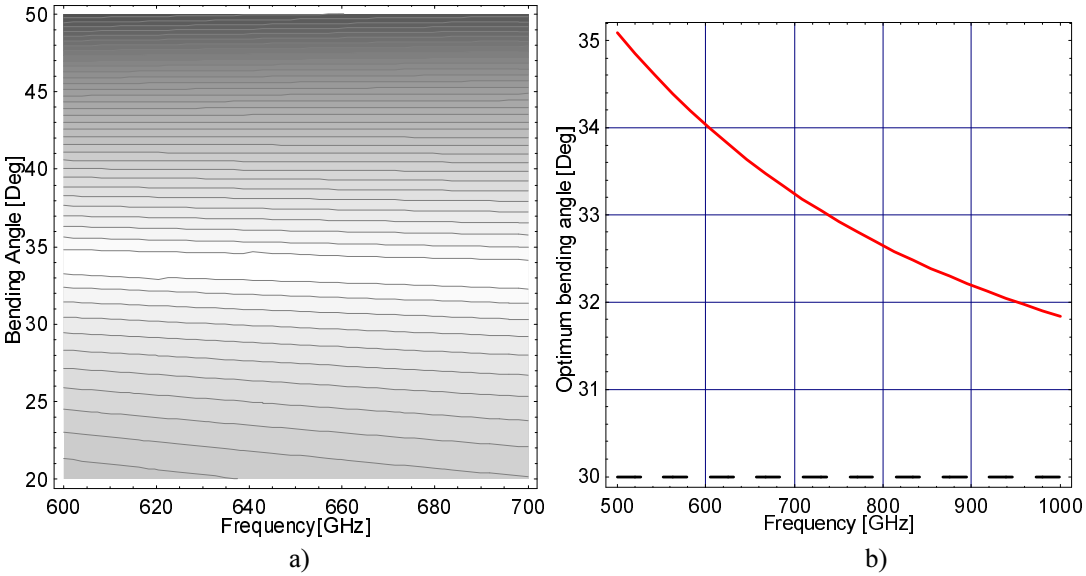

Figure 2.4 Losses due to distortion in pair of elliptical mirrors (a)). Distance between contours is 0.02 %. White area corresponds to losses less than 0.02 %. Optimal bending angle $\alpha 1$ vs. frequency when $\alpha 2$ is kept constant. $\alpha 2$ is calculated from (11) for $\alpha 1$=30°.

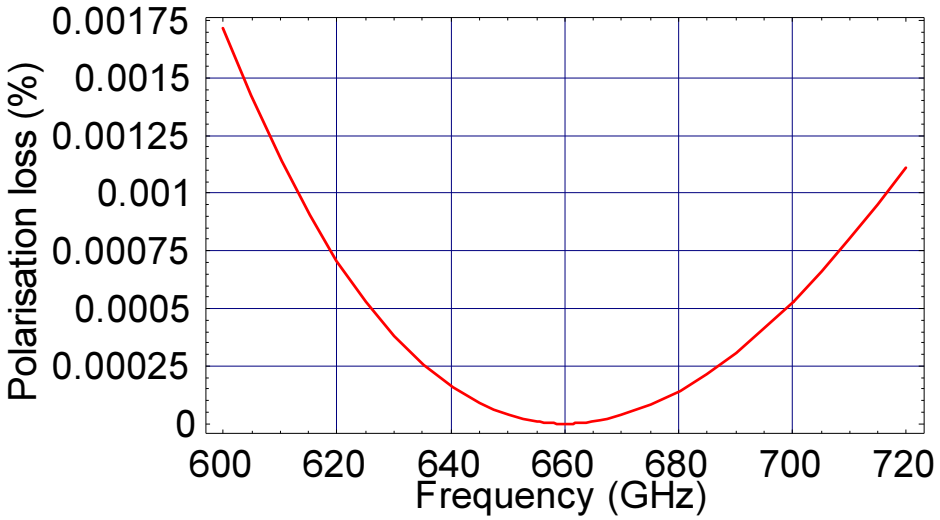

Figure 2.5 Cross-polarization loss in two-mirror system provided the correct choice of ellipses bending angles and focal distances.

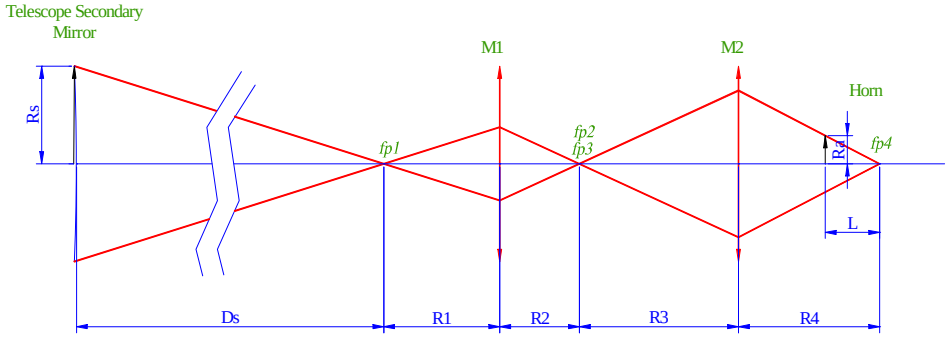

Figure 2.6 Optical train layout. Not in scale.

The result of calculation of losses for proposed two-mirror system is given in Figure 2.4 a). One can see that for each frequency the relation between bending angles becomes slightly different. The optimum angle is shown in Figure 2.4 b) compared to the geometrical limit optimum angle shown by dashed line. The cross-polarization loss for the case of compensated lens system is shown in Figure 2.5
The choice of final bending angles must be verified by using full fundamental beam mode propagation through the system.
As it appear from the similarity of equations (8) and (9), the cross-polarization losses of these mirrors are also compensated. The accuracy of the geometrical optics approach is increased if mirrors are in far field of correspondent beam waists.
The equation similar to (11) can be derived for systems with more mirrors and, therefore by proper choice of bending angles distortion and cross-polarization introduced by a feed offset can be fully or partially compensated.
The distortion compensation approach is being verified by propagating the fundamental Gaussian mode through various mirror systems in the framework of HIFI project. Preliminary results show good agreement.

2.3 Frequency independent coupling between horn and telescope beam

The optical train layout is shown in Figure 2.6. This is analogous to the layout shown in Figure 2.2. Two elliptical mirrors M1, M2 are used to match the beam from a telescope secondary mirror to a horn. We will discuss here the choice of mirror parameters (R1, R2, R3 and R4) for providing frequency independent coupling between telescope and mixer.
As it was discussed in section 2.1 the optimal fundamental Gaussian mode beam should have the radius of curvature equal to horn slant and at the same time it must have beam radius $Ra = 0.644a$ where a is horn radius. In order to achieve that we use the known properties of an optical system. If the system is arranged in such a way, that it reimages the pupil (in our case the secondary mirror) onto the

horn aperture with the required beam size and, at the same time, it reimages the focal point into the horn apex then beam radius of curvature and beam radius are independent on frequency. That allows to use geometrical optics relations to calculate main parameters of the system.

Above conditions can be satisfied by system of three mirrors. Two mirrors can determine the magnification of the system and the third mirror can be used as a field mirror, specifying the pupil image position at the aperture of the horn. However, for specific set of parameters field mirror is not necessary.

It can be shown, that based on two free parameters $R1$, $R4$ the other parameters of system can be calculated using following expressions:

$$R2 = \frac{\mathrm{R1}\cdot\left(\mathrm{R1}\cdot R4\cdot Ds\cdot K^2 - R1\cdot R4\cdot L - R4\cdot Ds\cdot K^2\cdot L\right)}{Ds\cdot\left(R4 + R1\cdot K\right)\cdot L},$$

$$R3 = \frac{R2}{R1}\frac{R4}{K}, \qquad K = \frac{L}{\mathrm{Ra}}\frac{Rs}{Ds}, \tag{13}$$

$$f1 = \left(R1^{-1} + R2^{-1}\right)^{-1}, \quad f2 = \left(R3^{-1} + R4^{-1}\right)^{-1},$$

where K is the system angle magnification, L is the horn length, $f1, f2$ are mirror focal distances. All other parameters are clear from Figure 2.6.

The beam radius at the horn aperture Ra can be adjusted to realize different edge illumination of telescope secondary mirror. The following expression can be to calculate Ra from edge taper Te (dB) and horn radius a:

$$Ra = 0.2185\cdot a\sqrt{Te}\,. \tag{14}$$

A fundamental mode Gaussian beam propagation trough the system calculated by using (13) is shown in Figure 2.7. Gaussian beams are shown for $1w$ and $2.5w$ beam radii, input and output distances ($R1$, $R4$) Mirrors should pass $5w$ diameter beam in order to reduce truncation losses. The calculation was done for lowest band frequency 600 GHz assuming that $R1 = 100$ mm, $R4 = 70$ mm and horn with parameters, described later in section 3.1.

The output waist position and size of this two-mirror system can be calculated using standard Gaussian optics formulae. As soon as a dependence of output beam waist position and size from frequency is known, equations (2), (3), (4) can be used to calculate final coupling between telescope and horn. Result of such calculation is presented in Figure 2.8 by solid line. The coupling appears to be frequency independent. The coupling for an equivalent Gaussian beam telescope system is shown in the same picture by the dashed line. It appears to be frequency dependent.

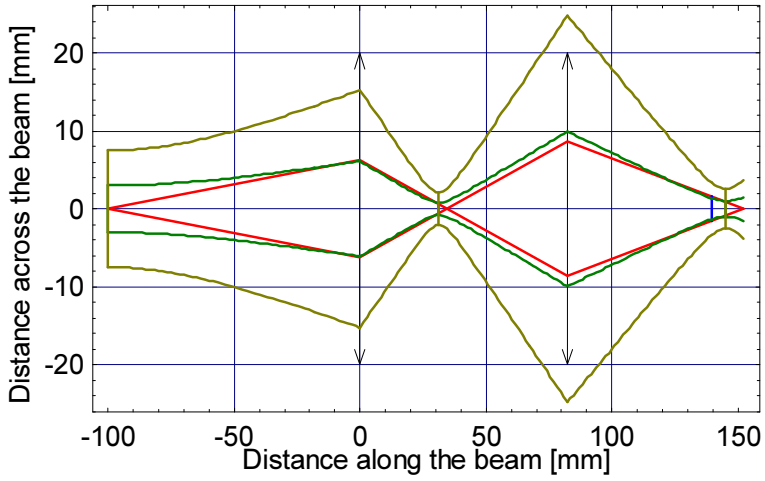

Figure 2.7 Optical train for a practical system. Gaussian beam contours for w and $2.5w$ radius are indicated as well as geometrical optics beam. Calculations were made for frequency 600 GHz and edge taper of 12 dB.

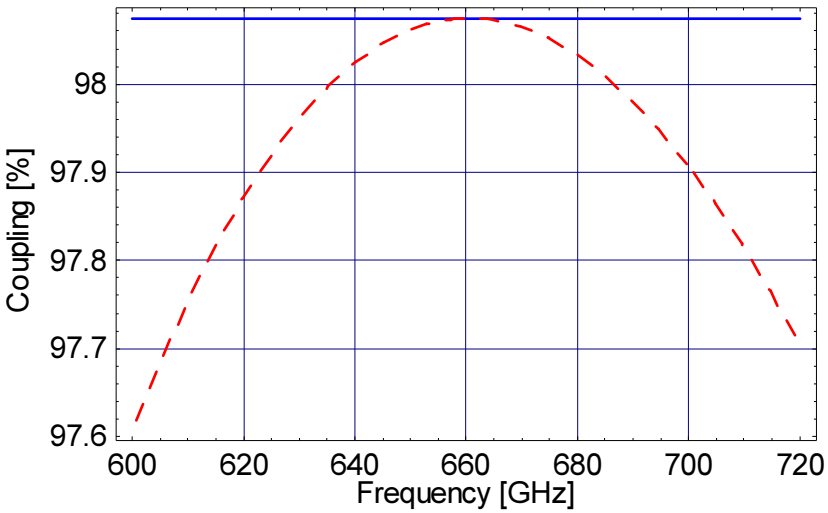

Figure 2.8 Optimized (solid line) and Gaussian beam telescope (dashed line) coupling between fundamental Gaussian mode beam illuminating the telescope secondary at 12 dB edge taper and a corrugated horn through two-mirror optical system.

3 Proposed layout

In this section we describe details of proposed two-mirror optical system. The detailed drawing of corrugated horn and parameters of an equivalent diagonal horn.

3.1 ALMA band 9 corrugated and diagonal horn design

The optimum corrugated horn design for ALMA band 9 is presented in Figure 3.1. This horn has the shortest slant length possible without degrading its antenna beam pattern. It allows to decrease amount of corrugations and makes the production easy. The optical parameters of this horn are:

Slant length:	12.867 mm
Aperture radius a_c:	2.1095 mm

The equivalent diagonal horn design is presented in Figure 3.2. As it was discussed in previous sections, these horns require the same waist size and position for optimum coupling to fundamental Gaussian beam mode. Optical parameters of this diagonal horn are:

Slant length:	12.867 mm
Aperture size a_r:	3.16 mm

For preliminary mixer design, an equivalent diagonal horn will be produced because of long delivery time of corrugated horns. We propose, that local oscillator (LO) output beam is also formed by a diagonal horn shown in Figure 3.2. This allows to minimize the production cost without decreasing significantly the coupling between local oscillator and mixer. In addition, if two the same diagonal horns are used for transmitting the LO signal and for receiving it the symmetrical mirror system can be used in-between and coupling could be even better than one predicted by Gaussian beam analysis.

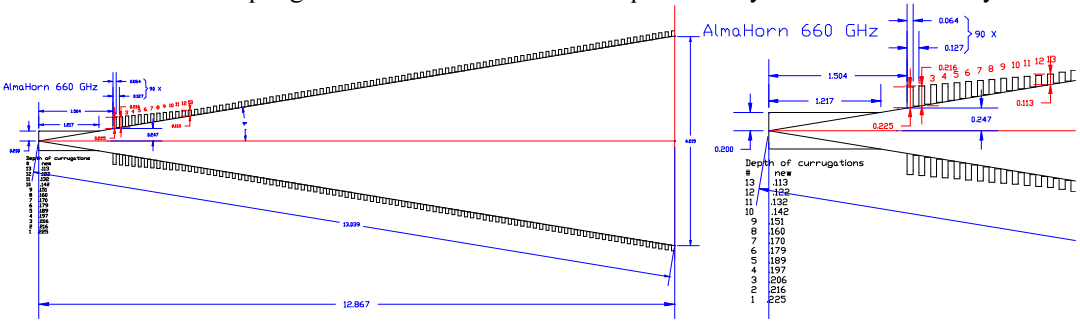

Figure 3.1 Optimum corrugated horn for 600-720 GHz

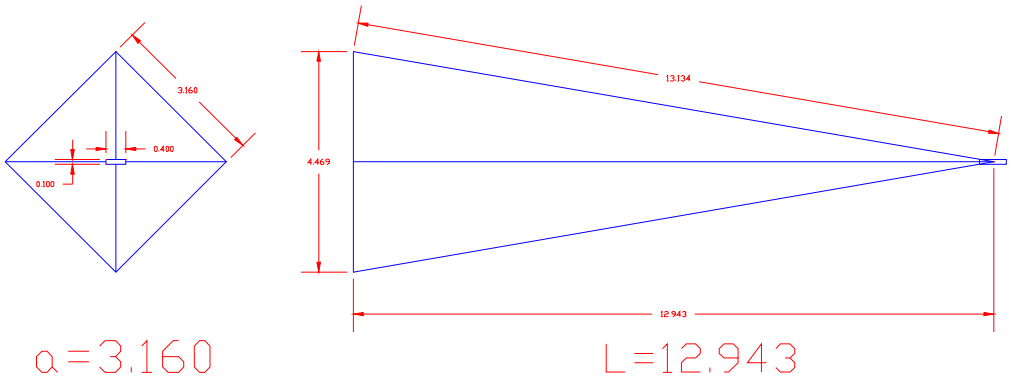

Figure 3.2 Diagonal horn, equivalent to corrugated horn shown in Figure 3.1

3.2 ALMA band 9 signal path optical layout

The proposed layout drawing is shown in Figure 3.3. The input signal comes from the top. The bending angle of the first ellipse is chosen to be 30°. One should note that if angles of two ellipses are related as described in section 2.2, the distortion appears to be compensated for any realizable bending angle of first mirror. Therefore this angle was chosen just to give enough space for dewar wall and radiation shields. This space is of order of 50 mm. The parameters of this design were calculated for 12 dB illumination of secondary mirror taking into account corrugated horn design described in previous session. Parameters of optical train are:

R1=100 mm, R2= 34.45 mm, R3= 47.88 mm, R4=70 mm, $f1$=25.62, $f2$=28.43

The loss in whole design is frequency independent and is less than 1%. Distortions and cross-polarization in two mirrors compensate so the associated loss should be less than 0.02 % for central frequency. This number should be still verified by a more accurate model. This design is physically smaller than a Gaussian beam telescope between the same horn and telescope focal plane.

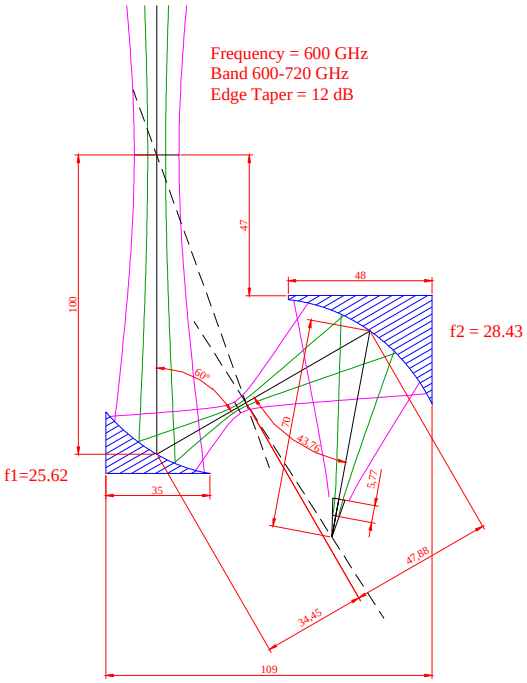

Figure 3.3 Proposed signal path layout calculated for lower band frequency (600 GHz). Input signal comes from the top. The small tilt angle due to cartridge offset in the telescope focal plane is not shown. Dashed lines indicate ellipses main axes.

4 Mirror alignment tolerances

In this section an individual mirror and horn alignment tolerances are considered. Some mirror offsets can be compensated or by refocusing (shift in the telescope secondary mirror) or by calibrating pointing offsets. Some facts that are stated in [4] were used.

Let us consider the offset of mirror M2 in the optical train while all other elements are kept in the same absolute position. The output waist position can be calculated by using ray matrices of elements. The dependence of optical coupling vs. mirror offset is shown in Figure 4.1. The tolerances for 1% of efficiency loss are maximal for highest frequency of 720 GHz and correspond to the range of –1.63 … 1.88 mm.

However, if one allow for a in change the distance between focal plane and first mirror (it can be achieved by adjustment of the telescope secondary mirror) the position tolerances of this mirror offset becomes much less critical: -2.3 … >3 (or even >14) mm. This is illustrated by Figure 4.2. The same considerations can be applied to all relative movements making tolerances less critical.

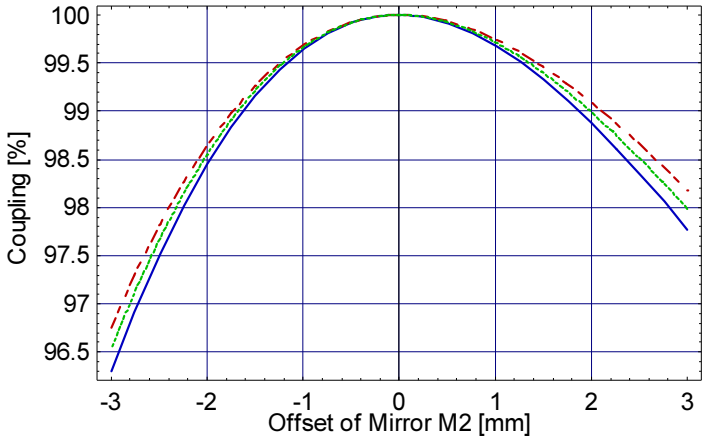

Figure 4.1 Coupling through the system vs. mirror M2 offset for different frequencies. Solid blue line corresponds to 600 GHz, dashed red line corresponds to 720 GHz, and dotted green line corresponds to 660 GHz.

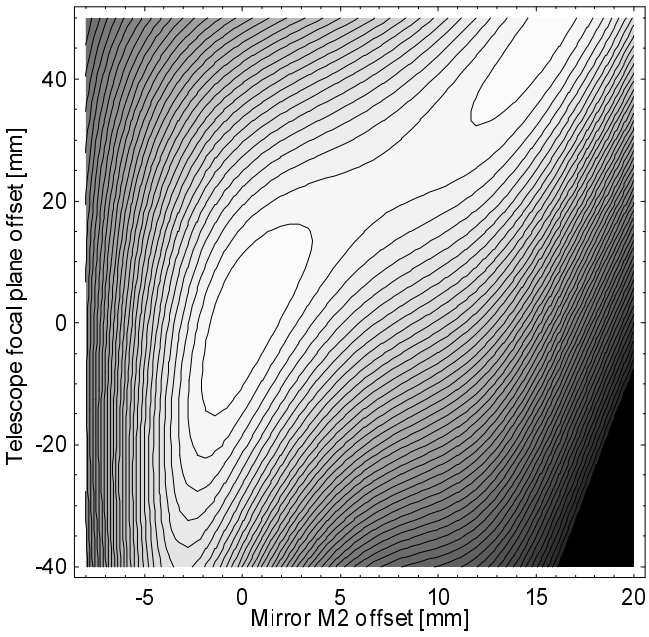

Figure 4.2 Optical coupling versus telescope focal plane offset and mirror M2 offset. Distance between contours is 1%. Central white area corresponds to 100%. Additional truncation is not taken into account.

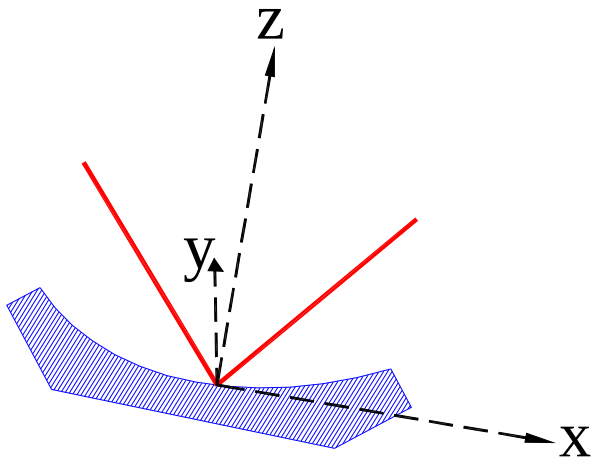

Figure 4.3 Local coordinate system used for mirror tolerance calculations. X- and z-axes are in the plane of the beams. Z-axis is perpendicular to the mirror surface.

For calculating of the actual alignment tolerances mirror bending angles should be taken in to account. Mirror offset can be described by shifts and rotations in three orthogonal axes as shown in Figure 4.3. The chief ray was propagated through the system and output waist offset due to movement of one mirror was calculated in the paraxial limit. Aberrations and distortions are not taken in to account in this calculation as an effect of second order. Results of calculations allowing for 1% of relative loss per degree of freedom are shown in table Table 1. The second column shows mirror/horn displacement when telescope secondary focus position is kept fixed. The third column shows the same tolerance provided that telescope can be defocused and focal plane offset is calibrated out. The fourth and fifth columns show optimized values and offsets. It can be seen that allowing for some adjustments makes some tolerances less strict. Most critical type of movement is therefore mirror rotations.

Table 1 Alignment tolerances budget

Misalignment type	Offset (non compensated)	Compensated offset	Defocus (mm)	Focal plane offset (mm)
Mirror offsets				
Mirror M1 x-axis offset	0.067 mm	0.157 mm	0.366	-0.528
Mirror M1 y-axis offset	0.058 mm	0.136 mm	0.366	-0.528
Mirror M1 z-axis offset	0.185 mm	0.260 mm	-1.19	0.252
Mirror M2 x-axis offset	0.045 mm	0.075 mm	0.352	0.331
Mirror M2 y-axis offset	0.041 mm	0.068 mm	0.352	0.331
Mirror M2 z-axis offset	0.423 mm	0.575 mm	-2.05	0.236
Mirror rotations				
Mirror M1 x-axis rotation	0.037 °	0.088 °	-0.303	-0.534
Mirror M1 y-axis rotation	0.065 °	0.153 °	-0.303	-0.534
Mirror M1 z-axis rotation	Inf	Inf	--	--
Mirror M2 x-axis rotation	0.028 °	0.044 °	-0.31	0.3
Mirror M2 y-axis rotation	0.051 °	0.081 °	-0.31	0.3
Mirror M2 z-axis rotation	Inf	Inf	--	--
Horn offsets				
Horn lateral offset	0.093 mm	0.137 mm	0.341	0.269
Offset along the beam	1.3 mm	1.3 mm	0.512	0
Horn rotations				
Horn tilt	0.817 °	1.11 °	0.188	-0.231
Rotation about beam axis	5.74 °	--	--	--

5 Conclusions

1) Proposed layout is frequency independent
2) It is possible to compensate for cross-polar and distortion losses in two (in more than two mirrors) and attempt is made to implement this into this layout
3) Alignment tolerances must be considered together with possibility of pointing offset and refocusing of the telescope.
4) Proposed layout is physically smaller than Gaussian beam telescope
5) The same idea of signal coupling can be applied to ALMA channels 6-10.

Acknowledgements

Authors thank James Lamb and Matt Carter for useful comments and discussions.

REFERENCES

[1] P. Golgsmith, "Quasioptical Systems"

[2] J. A. Murphy, "Distortion of a simple Gaussian beam on reflection from off-axis ellipsoid mirrors," *Int. J. Infrared and Millimeter Waves*, vol. **8**, no. 9, pp. 1165–87, 1988.

[3] H. van de Stadt, private communications

[4] B. Lazareff , "ALMA Optical tolerances report I and II"